Glucagon Receptor Signaling Regulates Energy Metabolism via Hepatic Farnesoid X Receptor and Fibroblast Growth Factor 21

Teayoun Kim,[1] Shelly Nason,[1] Cassie Holleman,[1] Mark Pepin,[2] Landon Wilson,[3] Taylor F. Berryhill,[3] Adam R. Wende,[2] Chad Steele,[4] Martin E. Young,[5] Stephen Barnes,[3] Daniel J. Drucker,[6] Brian Finan,[7] Richard DiMarchi,[7,8] Diego Perez-Tilve,[9] Matthias Tschöp,[10] and Kirk M. Habegger[1]

Diabetes 2018;67:1773–1782 | https://doi.org/10.2337/db17-1502

Glucagon, an essential regulator of glucose and lipid metabolism, also promotes weight loss, in part through potentiation of fibroblast growth factor 21 (FGF21) secretion. However, FGF21 is only a partial mediator of metabolic actions ensuing from glucagon receptor (GCGR) activation, prompting us to search for additional pathways. Intriguingly, chronic GCGR agonism increases plasma bile acid levels. We hypothesized that GCGR agonism regulates energy metabolism, at least in part, through farnesoid X receptor (FXR). To test this hypothesis, we studied whole-body and liver-specific FXR-knockout (*Fxr*$^{\Delta liver}$) mice. Chronic GCGR agonist (IUB288) administration in diet-induced obese (DIO) *Gcgr*, *Fgf21,* and *Fxr* whole-body or liver-specific knockout ($^{\Delta liver}$) mice failed to reduce body weight when compared with wild-type (WT) mice. IUB288 increased energy expenditure and respiration in DIO WT mice, but not *Fxr*$^{\Delta liver}$ mice. GCGR agonism increased [^{14}C]palmitate oxidation in hepatocytes isolated from WT mice in a dose-dependent manner, an effect blunted in hepatocytes from *Fxr*$^{\Delta liver}$ mice. Our data clearly demonstrate that control of whole-body energy expenditure by GCGR agonism requires intact FXR signaling in the liver. This heretofore-unappreciated aspect of glucagon biology has implications for the use of GCGR agonism in the therapy of metabolic disorders.

Glucagon is secreted from pancreatic α-cells in response to hypoglycemia and is the primary counterregulatory hormone to insulin action, increasing glycogenolysis and gluconeogenesis while simultaneously inhibiting glycogen synthesis (1). These actions, although beneficial in the context of hypoglycemia, may contribute to pathophysiological hyperglycemia in the setting of diabetes (2). Glucagon receptor (GCGR) agonism also modulates bile acid (BA) metabolism, stimulates fatty acid utilization, and reduces dyslipidemia, characteristics clearly desirable in antiobesity therapeutics (1). It is now accepted that GCGR agonism, when coupled with glucagon-like peptide 1 (GLP-1) agonism, offers potential opportunities for the therapy of metabolic syndrome (3,4).

We have reported that fibroblast growth factor 21 (FGF21), secreted in response to GCGR agonism, mediates many glucagon actions, including the prevention of diet-induced obesity (DIO) (5). Like glucagon, FGF21 regulates cholesterol (CHL) and BA metabolism (6,7).

[1]Comprehensive Diabetes Center and Division of Endocrinology, Diabetes and Metabolism, Department of Medicine, University of Alabama at Birmingham, Birmingham, AL
[2]Division of Molecular and Cellular Pathology, Department of Pathology, University of Alabama at Birmingham, AL
[3]Department of Pharmacology, University of Alabama at Birmingham, Birmingham, AL
[4]Division of Pulmonary, Allergy and Critical Care Medicine, Department of Medicine, University of Alabama at Birmingham, Birmingham, AL
[5]Division of Cardiovascular Disease, Department of Medicine, University of Alabama at Birmingham, Birmingham, AL
[6]Department of Medicine, Lunenfeld-Tanenbaum Research Institute, Sinai Health System, University of Toronto, Toronto, Ontario, Canada
[7]Novo Nordisk Research Center Indianapolis, Indianapolis, IN
[8]Department of Chemistry, Indiana University, Bloomington, IN
[9]Division of Endocrinology, Diabetes and Metabolism, Metabolic Diseases Institute, University of Cincinnati, Cincinnati, OH
[10]Institute for Diabetes and Obesity, Helmholtz Zentrum München, München, Germany

Corresponding author: Kirk M. Habegger, kirkhabegger@uabmc.edu.

Received 12 December 2017 and accepted 11 June 2018.

This article contains Supplementary Data online at http://diabetes.diabetesjournals.org/lookup/suppl/doi:10.2337/db17-1502/-/DC1.

Similarly, the BA nuclear receptor farnesoid X receptor (FXR) is a regulator of energy metabolism, mitochondrial function, and FGF21 gene expression (8). In this study, we investigated the roles of hepatic GCGR, FGF21, and FXR in the antiobesity effects of the GCGR agonist IUB288.

RESEARCH DESIGN AND METHODS

Animal Models

All studies were approved by and performed according to the guidelines of the Institutional Animal Care and Use Committee of the University of Alabama at Birmingham or the University of Cincinnati. Mice were single or group housed on a 12:12-h light/dark cycle at 22°C and constant humidity with free access to food and water, except as noted. *Gcgr*- and *Fxr*-floxed mice were obtained from the original investigators (9,10), whereas *Fgf21*-floxed and *Albumin*-Cre mice were obtained from The Jackson Laboratory (Bar Harbor, ME). All models were validated for tissue-specific, target gene knockout (Supplementary Fig. 1*A*–*E*). All mice maintained in our facilities are on a C57Bl/6J background. Mice were fed standard chow (5.8% fat; Teklad LM-485; Harlan Teklad) for colony maintenance and high-fat diet (HFD) (58.0 kcal% fat; D12331; Research Diets, New Brunswick, NJ) for DIO studies. For sacrifice, isoflurane anesthesia was used, torso blood was collected, and plasma was collected by centrifugation of whole blood at 3,000*g* for 10 min.

Peptides

IUB288 was synthesized as previously described (5) and native glucagon obtained from American Peptide Company.

Body Composition and Indirect Calorimetry

Body weight (BW) and food intake measurements were collected twice a week. Body composition was measured using MRS (EchoMRI; Echo Medical Systems). Combined indirect calorimetry was conducted as previously described (Comprehensive Lab Animal Monitoring System; Columbus Instruments) (11).

Glucose Tolerance Test

Intraperitoneal glucose (1.5 g/kg, 20% weight for volume D-glucose in 0.9% weight for volume saline; Sigma-Aldrich, St. Louis, MO) tolerance tests were conducted in 5-h–fasted mice as previously published (12). Tail vein blood glucose was assessed using a glucometer (Therasense FreeStyle glucometer; Abbott Laboratories, Abbott Park, IL).

Plasma and Tissue Analyses

Lipids in plasma and tissue samples from 2-h–fasted mice were determined using Infinity Triglycerides (#TR22421; Thermo Fisher Scientific), Infinity Cholesterol (#TR13421; Thermo Fisher Scientific), Total Bile Acids Assay Kit (#80259; Crystal Chem), and β-Hydroxybutyrate (Ketone Body) Colorimetric Assay Kit (#700190; Cayman Chemical).

BA Profiling

Plasma aliquots (50 μL) were extracted to recover BAs. Diluted extracts (1.25 μL plasma equivalent) were resolved by reverse-phase gradient liquid chromatography and analyzed by negative electrospray ionization mass spectrometry using multiple-reaction monitoring. BA peak areas were analyzed by MultiQuant 3.0.1 (SCIEX) and compared with peak-area concentration standard curves of individual BAs. Plasma hormones from 2-h–fasted mice were determined by Bio-Plex Pro Mouse Diabetes 8-Plex Assay (Bio-Rad Laboratories) in plasma samples collected in the presence of protease and phosphatase inhibitors (Halt; Thermo Fisher Scientific).

Quantitative Real-time PCR and RNA-Sequence Analysis

Liver RNA was isolated from 2-h–fasted mice using the RNeasy Lipid Mini-Kit (Qiagen, Valencia, CA), and cDNA was synthesized by RT-PCR using SuperScriptIII, DNase treatment, and anti-RNase treatment according to the manufacturer's instructions (Invitrogen, Carlsbad, CA). Single-gene quantitative PCR was performed as previously described (11). Data were normalized to housekeeping genes *Hprt*, *Rps18*, or *Ppia* using the ΔΔ threshold cycle calculation. See Supplementary Table 1 for a list of primer sets. High-throughput RNA sequencing was performed in the Heflin Genomics Core at the University of Alabama at Birmingham (UAB). Gene network associations and differentially expressed genes were identified via unpaired two-tailed and Bonferroni-adjusted *P* values (*Q* value) <0.05, respectively. Sequencing data have been deposited within the Gene Expression Omnibus repository (https://www.ncbi.nlm.nih.gov/geo). Gene set enrichment analysis, functional and network analyses, and candidate upstream regulators were identified via Qiagen's Ingenuity Pathway Analysis, where fold change >1.5, $P < 0.05$, and fragments per kilobase of transcript per million mapped reads >2.

Primary Hepatocyte Isolation

Primary hepatocytes were prepared from anesthetized mice as previously described (13). Perfusion (Krebs Ringer with glucose and 0.1 mmol/L EGTA) followed by digestion buffer (Krebs Ringer with glucose, 1.4 mmol/L $CaCl_2$, and 50 μg/mL liberase [05401119001; Roche]) was infused into the vena cava via peristaltic pump. Viable hepatocytes were recovered by Percoll gradient centrifugation (350*g* for 5 min) followed by washing (50*g* for 3 min, three times) and seeded on rat tail type 1 collagen-coated plates in DMEM (10% FBS and 1% penicillin/streptomycin) with all experiments conducted <24 h postisolation.

Statistics

All data are represented as mean ± SEM. Statistical significance was determined using unpaired Student *t* tests or, where appropriate, one- and two-way ANOVA with multiple-comparison Tukey and Sidak posttest, respectively. Statistics were completed using Prism version 7.0 for Macintosh and Windows (GraphPad Software, San Diego, CA). Statistical significance was assigned when *P* was <0.05.

RESULTS

Glucagon Promotes Body and Fat Mass Loss via Hepatic GCGRs

We have previously reported that GCGR agonism reduces body and fat mass in DIO mice (5). Considering the high level of *GcgR* expression in liver tissue, we reasoned that the antiobesity signal may be hepatic in origin and tested this hypothesis using mice deficient for hepatic *Gcgr* (*Gcgr*$^{\Delta liver}$) (9). Six- to 8-week-old male *Gcgr*$^{\Delta liver}$ mice and their littermate controls were placed on an HFD for 10 weeks to induce obesity. High-fat (HF) feeding stimulated similar food intake and accumulation of BW in both genotypes (Fig. 1*A* and *B*). *Gcgr*$^{\Delta liver}$ mice exhibited slightly less fat mass and a trend for more lean mass (Fig. 1*C*), with profoundly enhanced glucose tolerance as compared with their HF-fed littermate controls (Fig. 1*D*). Following HF feeding, mice were matched for BW and fat mass within each genotype and treated for 17 days with vehicle (saline) or IUB288 (10 nmol/kg/day). *Gcgr*$^{\Delta liver}$ mice were protected from hyperglycemia following GCGR agonism (Fig. 2*A*). Chronic GCGR agonism significantly reduced BW (Fig. 2*B* and Supplementary Fig. 1*F*) in wild-type (WT) mice, an effect mainly driven by fat mass loss with a modest decrease in lean mass (Fig. 2*C*). In contrast, BW, fat, and lean mass were preserved in IUB288-treated *Gcgr*$^{\Delta liver}$ mice (Fig. 2*B* and *C*). IUB288 treatment reduced food intake in both genotypes, yet food consumption was not different between *Gcgr*$^{\Delta liver}$ mice and their littermate controls (Fig. 2*D*).

We next examined the impact of GCGR agonism on circulating lipids. Chronic GCGR agonism significantly reduced circulating CHL in WT but not in *Gcgr*$^{\Delta liver}$ mice, with no effect on circulating triglycerides (TGs) (Fig. 2*E*). Conversely, chronic GCGR agonism significantly reduced hepatic TG levels in WT but not *Gcgr*$^{\Delta liver}$ mice, whereas liver CHL was unaffected by either genotype or treatment (Fig. 2*F*). Altogether, these data demonstrate the regulatory role of hepatic GCGR in whole-body energy balance, glucose, and lipid metabolism.

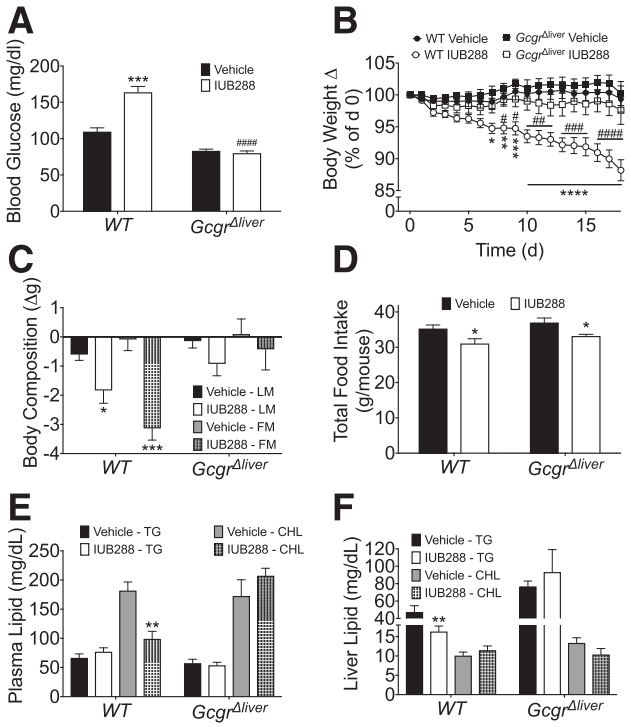

Figure 2—GCGR agonism in *Gcgr*$^{\Delta liver}$ mice. *A*: Ad libitum blood glucose of DIO WT and *Gcgr*$^{\Delta liver}$ mice (see Fig. 1) following daily GCGR agonism (10 nmol/kg IUB288). Change in percent BW (*B*) and body composition (*C*) after daily GCGR agonism. Total food intake (*D*), plasma (*E*), and liver (*F*) TG and CHL in DIO WT and *Gcgr*$^{\Delta liver}$ mice following daily GCGR agonism. All data are represented as mean ± SEM (n = 8–12 mice/group). *$P < 0.05$; **$P < 0.01$; ***$P < 0.001$; ****$P < 0.0001$, as compared with vehicle controls; #$P < 0.05$; ##$P < 0.01$; ###$P < 0.001$; ####$P < 0.0001$ as compared between genotypes within treatment. d, day; FM, fat mass; LM, lean mass.

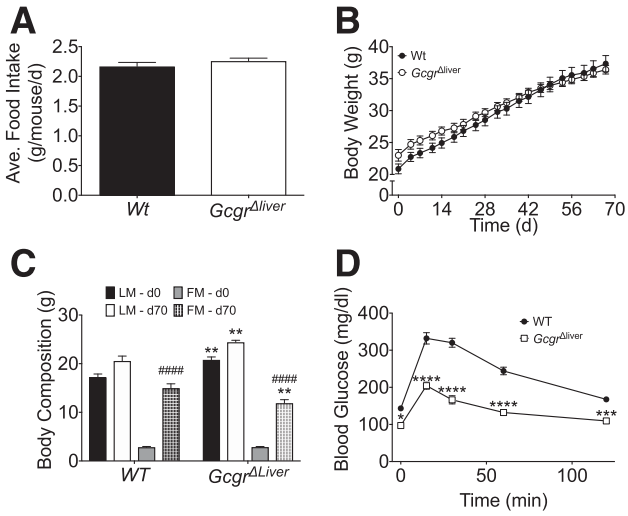

Figure 1—DIO in *Gcgr*$^{\Delta liver}$ mice. Average food intake (*A*) and absolute BW accrual (*B*) during 70 days (d) of HF feeding in male WT and *Gcgr*$^{\Delta liver}$ mice. *C*: Fat mass (FM) and lean mass (LM) of mice before (t = 0 day [d0]) and after (t = 70 days [d70]) HF feeding. *D*: Glucose tolerance of WT and *Gcgr*$^{\Delta liver}$ mice following 65 days of HF feeding. All data are represented as mean ± SEM (n = 17–23 mice/group). *$P < 0.05$; **$P < 0.01$; ***$P < 0.001$; ****$P < 0.0001$ as compared with littermate controls; ####$P < 0.0001$ as compared with baseline within genotype.

FGF21- and GCGR-Stimulated Obesity Reversal

We and others have reported that glucagon stimulates FGF21 secretion in hepatocytes (5,14). To address the role of FGF21, obesity was induced via 16 weeks of HF feeding in 20-week-old male, liver-specific, *Fgf21*-deficient (*Fgf21*$^{\Delta liver}$) and WT mice. Mice from each genotype were matched for BW and fat mass and treated for 16 days with vehicle (saline) or IUB288 (10 nmol/kg/day). Chronic GCGR agonism reduced BW (Fig. 3*A* and Supplementary Fig. 1*G*), food intake, and fat and lean mass in WT mice (Fig. 3*B* and *C*). However, BW reduction in *Fgf21*$^{\Delta liver}$ mice was significantly blunted, and GCGR-stimulated effects on body composition and food intake did not reach statistical significance (Fig. 3). Consistent

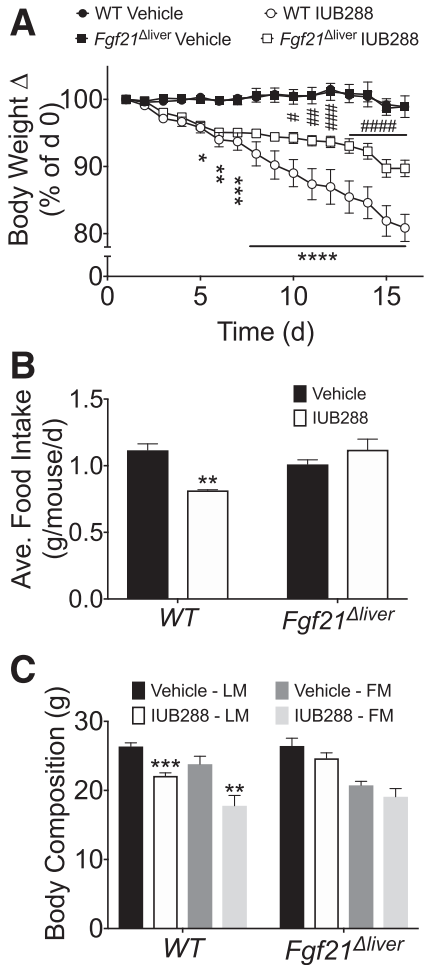

Figure 3—GCGR agonism in *Fgf21*$^{\Delta liver}$ mice. Change in percent BW (*A*), average food intake (*B*), and body composition (*C*) of 20-week-old male DIO WT and *Fgf21*$^{\Delta liver}$ mice following daily GCGR agonism (10 nmol/kg IUB288). All data are represented as mean ± SEM (n = 5–7 mice/group). Mice were maintained on an HFD for 12 weeks to induce DIO prior to treatment. *$P < 0.05$; **$P < 0.01$; ***$P < 0.001$; ****$P < 0.0001$, as compared with vehicle controls; #$P < 0.05$; ##$P < 0.01$; ###$P < 0.001$; ####$P < 0.0001$ as compared between genotypes within treatment. d, day; FM, fat mass; LM, lean mass.

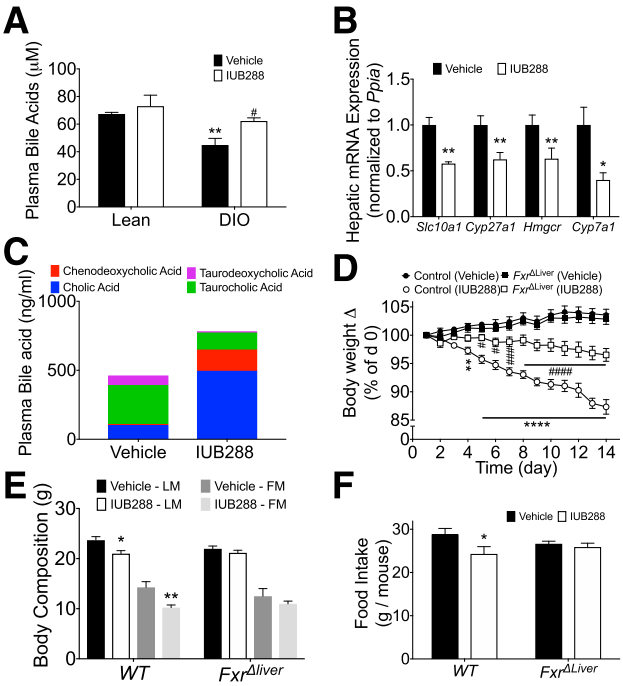

Figure 4—BA regulation and GCGR agonism in *Fxr*$^{\Delta liver}$ mice. *A*: Plasma BAs in male chow- and HF-fed C57Bl/6J mice following 18 days GCGR agonism (10 nmol/kg IUB288). *B*: Liver *Slc10a1*, *Cyp27a1*, *Hmgcr*, and *Cyp7a1* mRNA expression in DIO C57Bl/6J mice following 18 days GCGR agonism. *C*: Plasma BA profile in male WT mice following 16 days GCGR agonism. Change in percent BW (*D*), day 14 fat mass (FM) and lean mass (LM) (*E*), and food intake (*F*) of male DIO WT and *Fxr*$^{\Delta liver}$ mice following daily GCGR agonism (10 nmol/kg IUB288). All data are represented as mean ± SEM (n = 5–7 mice/group). WT and *Fxr*$^{\Delta liver}$ mice were placed on HFD at 8–10 weeks old and maintained on HFD for 10 weeks to induce DIO prior to treatment. *$P < 0.05$; **$P < 0.01$; ****$P < 0.0001$ as compared with vehicle controls; #$P < 0.05$; ###$P < 0.001$; ####$P < 0.0001$ as compared between genotypes/diet within treatment. d, day.

with our prior findings (5), these data suggest that FGF21-dependent and -independent mechanisms mediate body and fat mass loss following GCGR agonism.

FXR Mediates GCGR-Induced Body Weight Loss

Glucagon regulates BA metabolism (1), and BAs are known metabolic modulators (15). We sought to determine the contribution of BA metabolism in the effect of glucagon on BW. Circulating BAs are suppressed in DIO mice ($P <$ 0.01), yet rescued following chronic GCGR agonism (Fig. 4*A*), regulation that is absent in *Gcgr*$^{\Delta liver}$ mice (Supplementary Fig. 1*H*). IUB288 likewise reduced mRNA expression of BA regulators *Slc10a1*, *Cyp27a1*, *Hmgcr*, and *Cyp7a1* (Fig. 4*B*) (16) and elevated total and cholic BAs while decreasing taurodeoxycholic acids in DIO mice (Fig. 4*C*).

BAs are ligands of the FXR (FXR/Nr1h4) (15), leading us to investigate FXR signaling in glucagon action. Because both GCGR signaling (5) and FXR (8) are known to regulate *Fgf21* expression, we assessed hepatic *Fgf21* mRNA expression in response to GCGR agonist in WT and FXR-deficient (*Fxr*$^{-/-}$) mice. Intriguingly, hepatic gene expression and circulating levels of FGF21 were similarly upregulated in *Fxr*$^{-/-}$ and in WT control mice (Supplementary Fig. 2*A* and *B*) (two-way ANOVA, main effect of treatment, $P < 0.01$), suggesting GCGR agonism independently stimulates *Fxr* and *Fgf21* expression.

Six- to 8-week-old male WT and *Fxr*$^{-/-}$ mice were treated for 25 days with IUB288 concomitant with HF feeding to assess the role of FXR in GCGR-mediated prevention of HFD-induced metabolic defects. GCGR activation prevented HFD-induced BW and fat mass gain in WT but not in FXR-deficient mice (Supplementary Fig. 2*C*–*F*), whereas lean mass and food intake remained unaffected in this study (Supplementary Fig. 2*G* and *H*). These results indicate that FXR action is a necessary mediator of the GCGR signaling on BW.

Hepatic FXR Mediates GCGR-Stimulated Reduction in Obesity

Because our findings demonstrate that chronic glucagon action reduces BW via the liver, we generated liver-specific *Fxr*-knockout mice ($Fxr^{\Delta liver}$) to test the organ-specific contribution of FXR signaling. Six- to 8-week-old WT and $Fxr^{\Delta liver}$ mice exhibited similar BW and body composition while fed with standard chow (Supplementary Fig. 3*A*). However, $Fxr^{\Delta liver}$ mice were DIO resistant compared with WT mice (Supplementary Fig. 3*B*), despite similar caloric intake (Supplementary Fig. 3*C*). After the 10-week HF-feeding period, BW-matched mice from each genotype (WT, 38.3 ± 1.2 g; $Fxr^{\Delta liver}$, 35.3 ± 1.3 g) received daily injections of vehicle or the GCGR agonist. IUB288-treated WT mice lost 17% of their original BW ($P < 0.001$) (Fig. 4*D* and Supplementary Fig. 3*D*), including reductions of fat and lean mass (Fig. 4*E* and *F*). GCGR agonism increased intestinal, but not liver, *Gpbar1* mRNA expression in control but not $Fxr^{\Delta liver}$ mice (Supplementary Fig. 3*E*). Although GPBAR1/TGR5 signaling induces *Fgf21* (17) and Glp-1 (i.e., *Gcg*) (18), neither was differentially regulated in $Fxr^{\Delta liver}$ mice (Table 1 and Supplementary Fig. 1*A*, *B*, and *D*). IUB288 efficacy was blunted in $Fxr^{\Delta liver}$ mice, which lost significantly less BW when compared with IUB288-treated WT controls (Fig. 4*D* and Supplementary Fig. 3*D*). Furthermore, we failed to detect significant changes in either fat or lean mass in IUB288-treated $Fxr^{\Delta liver}$ mice compared with vehicle counterparts (Fig. 4*E*). Notably, WT IUB288-treated mice displayed a small (16%) reduction in food intake over the treatment period that was not observed in $Fxr^{\Delta liver}$ mice (Fig. 4*F*). The antiobesity effects of GCGR agonism were also associated with reduced epididymal and inguinal adipocyte size, as well as decreased lipid infiltration in brown adipose tissue (BAT) (Supplementary Fig. 4).

We assessed plasma samples from these mice to identify systems/pathways that were altered by GCGR agonism in an FXR-dependent manner (Table 1). Plasma GLP-1, insulin, plasminogen activator inhibitor 1, and glucagon levels were not altered by GCGR agonism. However, IUB288 treatment significantly decreased glucose-dependent insulinotropic polypeptide (GIP), leptin, and thyrotropin (TSH) levels in WT mice ($P < 0.05$), but not $Fxr^{\Delta liver}$ mice. Resistin and ghrelin levels were significantly decreased, whereas thyroxine (T4) (but not triiodothyronine [T3]) levels were significantly increased in both genotypes upon IUB288 treatment. Unlike WT mice, $Fxr^{\Delta liver}$ mice exhibit plasma BA accumulation as described (19) and were resistant to IUB288-induced regulation of BAs (Supplementary Fig. 3*F*). Together, these data highlight hepatic FXR as a critical mediator of glucagon's antiobesity action.

Hepatic FXR Mediates GCGR-Stimulated Increases in Energy Expenditure

To address mechanisms underlying the differential effects of GCGR agonism, we conducted indirect calorimetry in IUB288-treated $Fxr^{\Delta liver}$ and WT mice. Food intake was not significantly reduced by this short-term GCGR agonism (Supplementary Fig. 5*E* and *F*). Nonetheless, and consistent with our prior reports (5), BW reduction following GCGR agonism in DIO WT mice associated with an increase in light- and dark-phase energy expenditure (EE) (Fig. 5*A*, *B*, and *E* and Supplementary Fig. 5*A*). In contrast, IUB288 had no effect on EE in mice lacking hepatic FXR (Fig. 5*C–E* and Supplementary Fig. 5*B*). Likewise, GCGR agonism reduced respiratory quotient (RQ) in WT but not $Fxr^{\Delta liver}$ mice (Fig. 5*F* and *G* and Supplementary Fig. 5*C* and *D*), particularly during the light phase (Fig. 5*H*). Although EE was elevated in IUB288-treated WT mice, locomotor activity was not augmented by GCGR agonism in either genotype (Supplementary Fig. 5*G* and *H*). Altogether, these data suggest that GCGR agonism stimulates EE and fatty acid oxidation (FAOx), and this regulation is dependent upon hepatic FXR.

Table 1—Hormone profile in plasma samples

	WT vehicle	WT IUB288	$Fxr^{\Delta liver}$ vehicle	$Fxr^{\Delta liver}$ IUB288
Ghrelin (ng/mL)	30 ± 3.9	15 ± 1.4*	28 ± 3.4	15 ± 1.7**
GIP (pg/mL)	384 ± 62	183 ± 18*	314.7 ± 31.8	264 ± 37
GLP-1 (pg/mL)	38 ± 13	42.1 ± 14	48 ± 17	38 ± 13
PAI-1 (pg/mL)	809 ± 105	493 ± 22.5	856 ± 30.4	739 ± 136
Insulin (ng/mL)	5.4 ± 0.7	4.4 ± 0.5	4.5 ± 0.3	3.8 ± 0.3
Leptin (ng/mL)	12 ± 3	3.6 ± 0.9*	10.6 ± 1.5	3.0 ± 0.6
Glucagon (pg/mL)	272 ± 27	219 ± 20	303 ± 31	287 ± 19.5
Resistin (ng/mL)	109 ± 14	64 ± 8*	104 ± 6.5	62 ± 8.5*
TSH (ng/mL)	1.5 ± 0.1	0.8 ± 0.06*	1.5 ± 0.2	1.0 ± 0.1
T4 (ng/mL)	884 ± 59	1,520 ± 24****	607 ± 57##	1,320 ± 43****,#
T3 (ng/mL)	34 ± 1.8	40 ± 1	23 ± 1.3###	33 ± 2.1***,#

Data are mean ± SEM. $N = 7–10$/group. PAI-1, plasminogen activator inhibitor 1. *$P < 0.05$; **$P < 0.01$; ***$P < 0.001$; ****$P < 0.0001$ within genotype. #$P < 0.05$; ##$P < 0.01$; ###$P < 0.001$ between WT and $Fxr^{\Delta liver}$ in the same treatment.

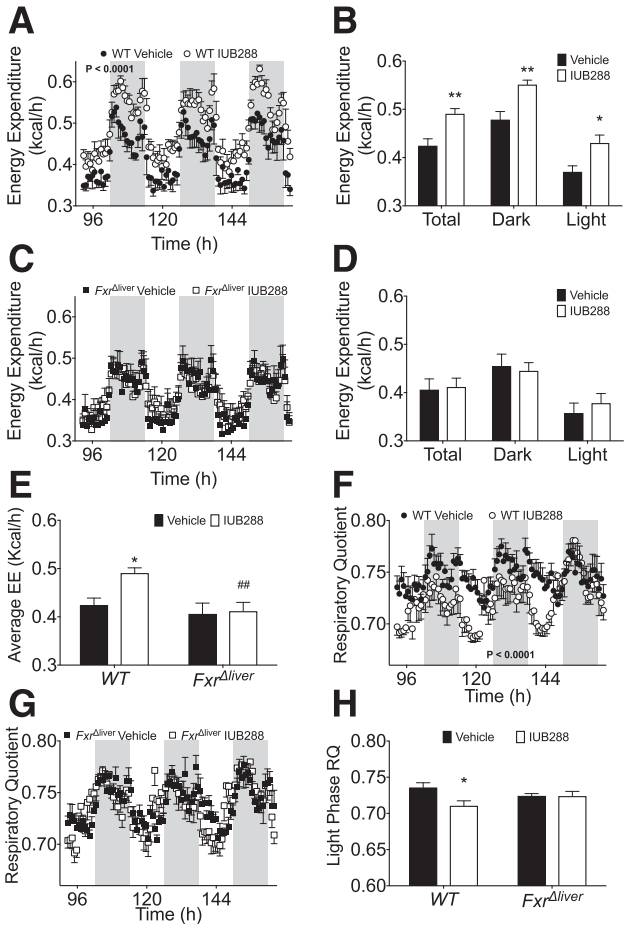

Figure 5—Indirect calorimetry during GCGR agonism in $Fxr^{\Delta liver}$ mice. EE (kcal/h) measured during final 72 h of 7 days indirect calorimetry analysis (*A* and *C*) and average diurnal EE (*B* and *D*) in DIO WT (*A* and *B*) and $Fxr^{\Delta liver}$ mice (*C* and *D*) during daily GCGR agonism (10 nmol/kg IUB288) of WT and $Fxr^{\Delta liver}$ mice (see Fig. 4). *E*: Average EE (final 72 h) in vehicle- and IUB288-treated mice. RQ during final 72 h (*F* and *G*) and light-phase RQ (*H*) in DIO WT and $Fxr^{\Delta liver}$ mice during daily GCGR agonism (10 nmol/kg IUB288). IUB288 administered via subcutaneous injection 1 h prior to dark phase (zeitgeber time [ZT]11). All data are represented as mean ± SEM (n = 6 mice/group). P values in *A* and *F* denote main effect of drug in repeated-measures two-way ANOVA. $^*P < 0.05$; $^{**}P < 0.01$ as compared with vehicle controls; $\#\#P < 0.01$ as compared between genotypes within treatment.

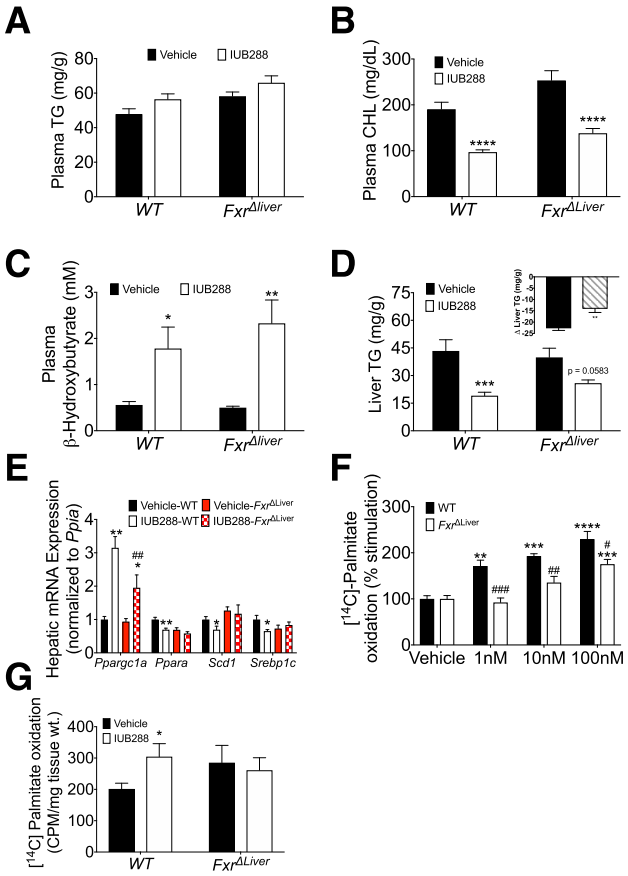

Figure 6—Liver lipid metabolism and FAOx during GCGR agonism in $Fxr^{\Delta liver}$ mice. Plasma TG (*A*), CHL (*B*), and β-hydroxybutyrate (*C*) in DIO WT and $Fxr^{\Delta liver}$ mice following 14 days of IUB288 treatment (see Fig. 4). Liver TG (*D*), change in liver TG (*D*, inset), and liver *Ppargc1a*, *Ppara*, *Scd1*, and *Srebp1c* mRNA expression (*E*) in 14-day IUB288-treated DIO WT and $Fxr^{\Delta liver}$ mice. *F*: [^{14}C]Palmitate oxidation in primary hepatocytes isolated from WT and $Fxr^{\Delta liver}$ mice and treated with IUB288 for overnight treatment followed by 3-h incubation with radioactive substrate in serum-free buffer. *G*: [^{14}C]Palmitate oxidation in liver tissue homogenates isolated from 6–8-month-old, chow-fed WT and $Fxr^{\Delta liver}$ mice following 2 days of IUB288 treatment (n = 4–6 mice/group). $^*P < 0.05$; $^{**}P < 0.01$; $^{***}P < 0.001$; $^{****}P < 0.0001$ as compared with vehicle controls; $\#P < 0.05$; $\#\#P < 0.01$; $\#\#\#P < 0.001$ as compared between genotypes within treatment. CPM, counts per minute.

Hepatic FXR Mediates GCGR Regulation of Hepatic Lipid Content and Oxidative Capacity

Plasma TGs trended higher after IUB288 treatment in both WT and $Fxr^{\Delta liver}$ mice (Fig. 6*A*). Conversely, plasma CHL was considerably reduced and plasma β-hydroxybutyrate was elevated by IUB288 treatment in both genotypes (Fig. 6*B* and *C*). As in previous studies (Fig. 2 and ref. 5), IUB288-treated WT mice exhibited significantly reduced hepatosteatosis, whereas this effect was blunted in $Fxr^{\Delta liver}$ mice (Fig. 6*D* and Supplementary Fig. 4). Consistent with a greater reduction in hepatic TG content, we also observed increased hepatic *Ppargc1a* expression concomitant with decreased *Ppara*, *Scd1*, and *Srebp1c* expression in WT mice, but not $Fxr^{\Delta liver}$ mice (Fig. 6*E*).

To elucidate potential pathways that may mediate the antiobesity action of the GCGR–FXR signaling axis, we conducted RNA-sequence analysis on liver samples from IUB288-treated WT and $Fxr^{\Delta liver}$ mice. This uncovered 953 genes differentially regulated by IUB288 treatment in an FXR-dependent manner, as well as 12 genes for which regulation was inverted in *Fxr* deficiency (Supplementary Fig. 6*A* and *B*). Top gene ontology–enriched pathways included oxidative phosphorylation, Eif2, p70S6K, sirtuin, and mammalian target of rapamycin signaling (Fig. 7*A*). Chip-sequencing enrichment analysis (20) of our data set identified retinoid X receptor (RXR), liver X receptor (LXR), and peroxisome proliferator–activated receptor α (PPARα) as likely upstream regulators (Fig. 7*B*). This analysis uncovered that genes related

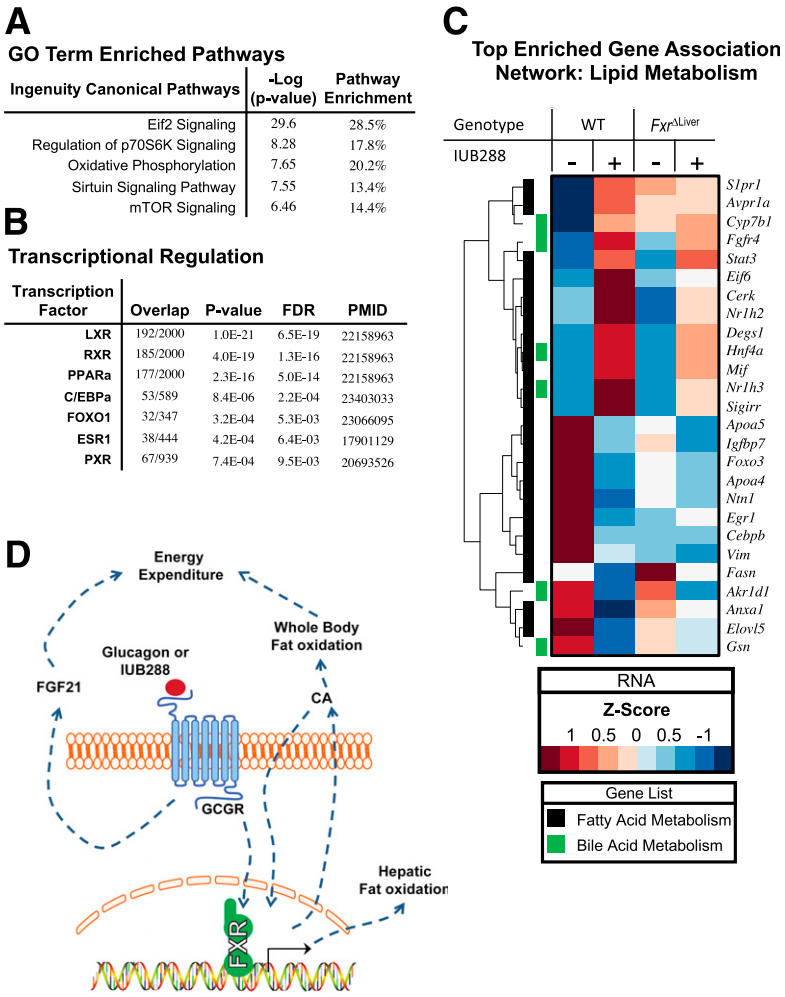

Figure 7—Transcriptional regulation stimulated by IUB288 treatment in $Fxr^{\Delta liver}$ and WT mice. *A*: Gene set enrichment analysis of the 953 genes differentially expressed only in the IUB288-treated WT vs. vehicle-treated WT was used to generate top five gene ontology (GO) term-enriched pathways. *B*: Published chromatin immunoprecipitation–sequencing data sets were used to enrich the genes exclusively regulated in WT mice. *C*: FXR-dependent differentially expressed genes associated with fatty acid or BA metabolism. Liver tissues analyzed from mice in Fig. 4. *D*: Proposed model of mechanisms regulating the antiobesity effects of glucagon-receptor agonism. CA, cholic acid; FDR, false discovery rate; LXR, liver X receptor; mTOR, mammalian target of rapamycin; PMID, PubMed identification number; PPARa, peroxisome proliferator–activated receptor α; PXR, pregnane X receptor; RXR, retinoid X receptor.

to BA (e.g., *Cyp7b1*, *Fgfr4*, and *Nr1h3*) and fatty acid metabolism (e.g., *Nr1h2*, *Fasn*, and *Apoa4*) were significantly regulated by GCGR activation (Fig. 7*C*). Consistent with a cell-autonomous FXR-dependent regulation, IUB288 or glucagon treatment stimulated FAOx in WT primary hepatocytes, but this activation was blunted in hepatocytes from $Fxr^{\Delta liver}$ mice (Fig. 6*F* and Supplementary Fig. 6*C*). Likewise, liver homogenates from WT mice previously treated with IUB288 displayed enhanced FAOx when compared with vehicle-treated controls, whereas this effect is lost in liver homogenates from IUB288-treated $Fxr^{\Delta liver}$ mice (Fig. 6*G*).

DISCUSSION

Glucagon, and by extension GCGR signaling, is a potent regulator of energy balance and glucose and lipid metabolism (1). Attempts to antagonize this critical metabolic pathway and thus reverse hyperglycemia have resulted in unexpected dyslipidemia, questioning whether attenuating or enhancing glucagon action is the appropriate therapeutic approach (21,22). Thus, an important and emerging question revolves around the identification of downstream mechanisms mediating GCGR action and potential segregation of GCGR-induced hyperglycemia from its antiobesity actions. In this study, we have investigated the thermogenic and antiobesity effects of GCGR signaling using IUB288 (5). We identified liver as the tissue of origin for these effects, demonstrating a role for FGF21 as a downstream regulator, and uncovered FXR signaling as an additional pathway that mediates some of the antiobesity actions of GCGR agonism. We likewise identified increased hepatocyte FAOx as a downstream action stimulated by GCGR agonism in an FXR-dependent manner. We further investigated the contributions of GCGR-mediated

regulation of BA metabolism, a crucial regulator of whole-body energy balance.

A Hepatic Antiobesity Signal

Whole-body germline disruption (23) or tamoxifen-induced conditional whole-body loss of GCGR (24) function results in protection from DIO upon HFD feeding. Interestingly, our data demonstrate that mice with congenital loss of hepatic *Gcgr* expression were not protected from DIO. Nonetheless, our results demonstrate that IUB288-stimulated BW loss in HFD-fed mice requires intact hepatic *Gcgr* expression. Although it is possible that hypothalamic, GCGR-dependent inhibition of food intake (25) or secondary effects of hepatic factors in other tissues, such as BAT and white adipose tissue (WAT), could be contributing to the weight loss, our observations suggest that GCGR-increased EE is predominantly due to a hepatic effect.

As with its antiobesity effects, the beneficial effects of GCGR signaling on dyslipidemia are well known (1); however, our studies clearly identify hepatic GCGRs as the drivers of reduced plasma CHL and liver TGs. It is important to note that lack of hepatic GCGR signaling is sufficient to drive increased hepatic TG accumulation and is consistent with increased dyslipidemia following GCGR antagonism (26). These data highlight both the potential for GCGR agonists as anti–nonalcoholic fatty liver disease therapeutics as well as cautioning against GCGR antagonism.

FGF21 as a Downstream Mediator of GCGR's Antiobesity Effect

We previously identified the hepatokine FGF21 as a crucial factor in GCGR-mediated energy metabolism (5). FGF21 null mice fail to respond to GCGR-stimulated prevention of DIO (5). However, in this study, HF feeding was initiated concurrent with GCGR agonism, and thus, FGF21 was only tested in the context of obesity prevention. In this paradigm, FGF21 was responsible for the entirety of GCGR-mediated energy balance. However, when these studies were moved to an obesity treatment paradigm, a more complex regulatory network emerged. These new studies in an obese model of liver FGF21 deficiency clearly show a blunted BW response to chronic GCGR agonism. It is possible that in pre-existing obesity, GCGR agonism stimulates FGF21 secretion from extrahepatic tissues. However, our findings in $Gcgr^{\Delta liver}$ mice support reports suggesting that the vast majority of circulating FGF21 is hepatically derived (27). Thus, we can surmise that if FGF21 is an important downstream regulator of GCGR action, it must be hepatic in origin. Although FGF21 is a potent antiobesity signal, it is clear that in the context of GCGR signaling, there are both FGF21-dependent and -independent pathways engaged, and we must look beyond the FGF21 signaling pathway.

FXR as a Parallel GCGR Signaling Pathway

Glucagon, via cAMP-dependent protein kinase–dependent regulation of HNF4α, modulates hepatocyte *Cyp7a1* expression, the rate-limiting enzyme in BA synthesis (28). Although this would predictably result in suppression of BA synthesis, we also observed suppression of *Slc10a* in IUB288-treated mice. Thus, it is possible that the elevated levels of BAs observed in circulation are the result, at least in part, of reduced hepatocyte transport at the basolateral membrane (29). Interruption of GCGR signaling (genetic or pharmacological) elevates primary and secondary plasma BAs (9,26,30,31). As compensatory effects of either genetic ablation or pharmacology could underlie these effects, our strategy to combine genetic and pharmacological interventions may provide a more complete view of these GCGR effects. Moreover, fasting, which was not controlled for in the cited reports (9,26,30,31), has a profound effect on BA levels.

We observed an elevation in the cholic acid species of BAs after GCGR agonism. This species is a potent activator of FXR (32) and suggests that glucagon signaling may regulate FXR signaling via BA metabolism. The interplay between BAs and FXR in the regulation of EE has yet to be fully elucidated. BAs increase EE in humans and rodent models of obesity (33–36), but these effects are often attributed to GPBAR1/TGR5, not FXR (37). Of interest, we observed an FXR-dependent increase in intestinal *Gpbar1* expression following GCGR agonism, providing a line of future focus. Conversely, BA-binding resins reduce serum BAs and are effective to prevent and treat DIO (38). Likewise, $Fxr^{-/-}$ mice are resistant to DIO (39). Consistent with this observation, chronic treatment with a synthetic FXR agonist GW4063 accentuated DIO (40), whereas FXR inhibition via tauro-β-muricholic acid (41) or glycine-β-muricholic acid (42) correlates with improved metabolic function. Thus, the role of BAs, FXR, and GPBAR1/TGR5 signaling in metabolic regulation warrants continued investigation.

Both GCGR (5) and FXR signaling (8) regulate the expression of FGF21. In this study, we report similar *Fgf21* expression and circulating FGF21 levels in $Fxr^{-/-}$, $Fxr^{\Delta liver}$, and WT control mice, demonstrating that FXR signaling is dispensable for GCGR-induced FGF21. Therefore, it is plausible that the intermediate effect on BW observed in both $Fgf21^{\Delta liver}$ and $Fxr^{\Delta liver}$ mice, as compared with their appropriate controls, is a reciprocal component of the GCGR effect. Although not directly tested in this study, studies are underway to assess the combined contributions of these two pathways. We also assayed endocrine pathways known to regulate energy balance (i.e., ghrelin, GIP, leptin, resistin, TSH, T3, and T4). However, all of these factors were regulated in a similar manner between WT and $Fxr^{\Delta liver}$ mice. This suggests that the liver is largely responsible for the FXR-dependent metabolic actions observed during GCGR agonism. Beyond FXR, GCGR activation may increase whole-body EE in part via thyroid hormone. Moreover, increased T4 levels are likely suppressing TSH in these mice. The suppressed ghrelin observed was a bit unexpected, as glucagon administration on isolated rat stomach has been reported to increase ghrelin secretion (43).

Whether the observed decrease in ghrelin levels contributes to IUB288-induced BW loss cannot be completely discarded based on our experiments.

Hepatic FXR as a Regulator of Whole-Body and Hepatic Energetics

Glucagon increases oxygen consumption, body temperature, and EE in rodents (5,43) and likewise increases EE and fat oxidation in humans (44,45). Similarly, FXR regulates EE (46) and mitochondrial function (47). Our studies suggest that at least a portion of glucagon's antiobesity action is mediated via hepatic FXR and involves an increase in EE. Consistent with accumulation of circulating IUB288 (an acylated peptide), EE increased with each subsequent dose and was most evident in the final days of indirect calorimetry. DIO $Fxr^{\Delta liver}$ mice were unresponsive to GCGR agonism, even after 5 days of treatment. Moreover, increased EE was independent of changes in locomotor activity, suggesting that GCGR agonism stimulates basal metabolic rate in an FXR-dependent manner. Substrate preference (RQ) was also altered by GCGR agonism. RQ in all mice was suppressed (~0.74) and indicative of the HF feeding. However, GCGR agonism was sufficient to further reduce RQ in WT but not $Fxr^{\Delta liver}$ mice, suggesting that GCGR signaling stimulates FAOx in an FXR-dependent manner. This, along with the potent reduction in fat mass observed after IUB288 treatment, also suggests that the energetic demands induced by GCGR agonism are met via increased FAOx. Lipolysis may represent one of the main effects of GCGR activation (i.e., to fuel fat utilization). The amount of free fatty acid released from BAT by glucagon treatment is 10 times higher than that of WAT (48). Therefore, it is plausible that BAT intracellular lipid provides the first source for glucagon-stimulated FAOx, whereas WAT may represent a later source. Studies are currently underway to address these questions; however, the results described in this study confirm prior reports that GCGR agonism stimulates hepatocyte FAOx (49). Regarding the mechanisms underlying this elevated oxidative state, we observed an increase in expression of hepatic oxidative phosphorylation genes and specifically *Ppargc1a*. Of note, overexpression of hepatic peroxisome proliferator–activated receptor γ coactivator 1α is sufficient to increase hepatic mitochondrial respiration and whole-body fat oxidation (50), suggesting that this critical transcriptional coregulator may also contribute to FAOx and fat mass loss in our system. Likewise, elevated cAMP (as in GCGR signaling) and *Ppargc1a* overexpression both induce *Fxr* (51). Furthermore, peroxisome proliferator–activated receptor γ coactivator 1α interacts with the FXR DNA-binding domain to enhance subsequent FXR target gene induction (51). Thus, future studies will focus on the interaction of these crucial transcriptional regulators in the context of GCGR signaling.

In conclusion, we report that hepatic FXR is a critical regulator of glucagon's antiobesity effects. The metabolic benefits of IUB288 appear to be liver cell autonomous, GCGR dependent, and mediated through parallel FGF21 and FXR pathways (Fig. 7*D*). These discoveries serve to further highlight the emerging value of fasting hormone pathways as superior target pathways for the treatment of metabolic disease. Additional dissection of the detailed molecular interactions connecting GCGR activation with FXR signaling and FGF21 induction may provide novel drug targets for the treatment of metabolic diseases.

Funding. The project described was supported by National Institutes of Health National Institute of Diabetes and Digestive and Kidney Diseases grants 5K01-DK-098319 and 1R01-DK-112934 (to K.M.H.), R01-DK-077975 (to D.P.-T.), and P30-DK-079626, as well as the UAB Small Animal Phenotyping Core supported by the National Institutes of Health Nutrition Obesity Research Centers (P30-DK-056336), Diabetes Research Center (P30-DK-079626), and the UAB Nathan Shock Center (PAG-050886A). This work was also supported by American Diabetes Association grant 1-13-JF-21 (K.M.H.), Canadian Institutes of Health Research grants 136942 and 154321, and the Canada Research Chairs Program (to D.J.D.).

Duality of Interest. No potential conflicts of interest relevant to this article were reported.

Author Contributions. T.K., S.N., C.H., L.W., T.F.B., and C.S. generated experimental data. T.K. and K.M.H. were responsible for study conception and design, data analyses and interpretation, and drafting the article. M.P. and A.R.W. were responsible for RNA-sequencing analyses. M.E.Y., S.B., D.J.D., B.F., R.D., D.P.-T., and M.T. advised on study concept and critical revision of the article. K.M.H. is the guarantor of this work and, as such, had full access to all of the data in the study and takes responsibility for the integrity of the data and the accuracy of the data analysis.

Prior Presentation. Parts of this study were presented at the 76th Scientific Sessions of the American Diabetes Association, New Orleans, LA, 10–14 June 2016, and the 77th Scientific Sessions of the American Diabetes Association, San Diego, CA, 9–13 June 2017.

References

1. Habegger KM, Heppner KM, Geary N, Bartness TJ, DiMarchi R, Tschöp MH. The metabolic actions of glucagon revisited. Nat Rev Endocrinol 2010;6:689–697
2. Brown RJ, Sinaii N, Rother KI. Too much glucagon, too little insulin: time course of pancreatic islet dysfunction in new-onset type 1 diabetes. Diabetes Care 2008;31:1403–1404
3. Day JW, Ottaway N, Patterson JT, et al. A new glucagon and GLP-1 co-agonist eliminates obesity in rodents. Nat Chem Biol 2009;5:749–757
4. Finan B, Yang B, Ottaway N, et al. A rationally designed monomeric peptide triagonist corrects obesity and diabetes in rodents. Nat Med 2015;21:27–36
5. Habegger KM, Stemmer K, Cheng C, et al. Fibroblast growth factor 21 mediates specific glucagon actions. Diabetes 2013;62:1453–1463
6. Kharitonenkov A, Shiyanova TL, Koester A, et al. FGF-21 as a novel metabolic regulator. J Clin Invest 2005;115:1627–1635
7. Ito S, Fujimori T, Furuya A, Satoh J, Nabeshima Y, Nabeshima Y. Impaired negative feedback suppression of bile acid synthesis in mice lacking betaKlotho. J Clin Invest 2005;115:2202–2208
8. Cyphert HA, Ge X, Kohan AB, Salati LM, Zhang Y, Hillgartner FB. Activation of the farnesoid X receptor induces hepatic expression and secretion of fibroblast growth factor 21. J Biol Chem 2012;287:25123–25138
9. Longuet C, Robledo AM, Dean ED, et al. Liver-specific disruption of the murine glucagon receptor produces α-cell hyperplasia: evidence for a circulating α-cell growth factor. Diabetes 2013;62:1196–1205
10. Sinal CJ, Tohkin M, Miyata M, Ward JM, Lambert G, Gonzalez FJ. Targeted disruption of the nuclear receptor FXR/BAR impairs bile acid and lipid homeostasis. Cell 2000;102:731–744
11. Loyd C, Liu Y, Kim T, et al. LDB1 regulates energy homeostasis during diet-induced obesity. Endocrinology 2017;158:1289–1297

12. Kirchner H, Hofmann SM, Fischer-Rosinský A, et al. Caloric restriction chronically impairs metabolic programming in mice. Diabetes 2012;61:2734–2742
13. Li WC, Ralphs KL, Tosh D. Isolation and culture of adult mouse hepatocytes. Methods Mol Biol 2010;633:185–196
14. Cyphert HA, Alonge KM, Ippagunta SM, Hillgartner FB. Glucagon stimulates hepatic FGF21 secretion through a PKA- and EPAC-dependent posttranscriptional mechanism. PLoS One 2014;9:e94996
15. Chiang JY. Bile acid metabolism and signaling. Compr Physiol 2013;3:1191–1212
16. Chiang JY. Regulation of bile acid synthesis: pathways, nuclear receptors, and mechanisms. J Hepatol 2004;40:539–551
17. Donepudi AC, Boehme S, Li F, Chiang JY. G-protein-coupled bile acid receptor plays a key role in bile acid metabolism and fasting-induced hepatic steatosis in mice. Hepatology 2017;65:813–827
18. Katsuma S, Hirasawa A, Tsujimoto G. Bile acids promote glucagon-like peptide-1 secretion through TGR5 in a murine enteroendocrine cell line STC-1. Biochem Biophys Res Commun 2005;329:386–390
19. Kim I, Ahn SH, Inagaki T, et al. Differential regulation of bile acid homeostasis by the farnesoid X receptor in liver and intestine. J Lipid Res 2007;48:2664–2672
20. Lachmann A, Xu H, Krishnan J, Berger SI, Mazloom AR, Ma'ayan A. ChEA: transcription factor regulation inferred from integrating genome-wide ChIP-X experiments. Bioinformatics 2010;26:2438–2444
21. Campbell JE, Drucker DJ. Islet α cells and glucagon–critical regulators of energy homeostasis. Nat Rev Endocrinol 2015;11:329–338
22. Unger RH, Cherrington AD. Glucagonocentric restructuring of diabetes: a pathophysiologic and therapeutic makeover. J Clin Invest 2012;122:4–12
23. Conarello SL, Jiang G, Mu J, et al. Glucagon receptor knockout mice are resistant to diet-induced obesity and streptozotocin-mediated beta cell loss and hyperglycaemia. Diabetologia 2007;50:142–150
24. Finan B, Clemmensen C, Zhu Z, et al. Chemical hybridization of glucagon and thyroid hormone optimizes therapeutic impact for metabolic disease. Cell 2016;167:843–857.e814
25. Quiñones M, Al-Massadi O, Gallego R, et al. Hypothalamic CaMKKβ mediates glucagon anorectic effect and its diet-induced resistance. Mol Metab 2015;4:961–970
26. Guan HP, Yang X, Lu K, et al. Glucagon receptor antagonism induces increased cholesterol absorption. J Lipid Res 2015;56:2183–2195
27. Markan KR, Naber MC, Ameka MK, et al. Circulating FGF21 is liver derived and enhances glucose uptake during refeeding and overfeeding. Diabetes 2014;63:4057–4063
28. Song KH, Chiang JY. Glucagon and cAMP inhibit cholesterol 7alpha-hydroxylase (CYP7A1) gene expression in human hepatocytes: discordant regulation of bile acid synthesis and gluconeogenesis. Hepatology 2006;43:117–125
29. Anwer MS, Stieger B. Sodium-dependent bile salt transporters of the SLC10A transporter family: more than solute transporters. Pflugers Arch 2014;466:77–89
30. Yang J, MacDougall ML, McDowell MT, et al. Polyomic profiling reveals significant hepatic metabolic alterations in glucagon-receptor (GCGR) knockout mice: implications on anti-glucagon therapies for diabetes. BMC Genomics 2011;12:281
31. Dean ED, Li M, Prasad N, et al. Interrupted glucagon signaling reveals hepatic α cell axis and role for L-glutamine in α cell proliferation. Cell Metab 2017;25:1362–1373.e5
32. Sepe V, Festa C, Renga B, et al. Insights on FXR selective modulation. Speculation on bile acid chemical space in the discovery of potent and selective agonists. Sci Rep 2016;6:19008
33. Broeders EP, Nascimento EB, Havekes B, et al. The bile acid chenodeoxycholic acid increases human brown adipose tissue activity. Cell Metab 2015;22:418–426
34. Chen X, Yan L, Guo Z, et al. Chenodeoxycholic acid attenuates high-fat diet-induced obesity and hyperglycemia via the G protein-coupled bile acid receptor 1 and proliferator-activated receptor γ pathway. Exp Ther Med 2017;14:5305–5312
35. Teodoro JS, Zouhar P, Flachs P, et al. Enhancement of brown fat thermogenesis using chenodeoxycholic acid in mice. Int J Obes 2014;38:1027–1034
36. Zietak M, Kozak LP. Bile acids induce uncoupling protein 1-dependent thermogenesis and stimulate energy expenditure at thermoneutrality in mice. Am J Physiol Endocrinol Metab 2016;310:E346–E354
37. Watanabe M, Houten SM, Mataki C, et al. Bile acids induce energy expenditure by promoting intracellular thyroid hormone activation. Nature 2006;439:484–489
38. Kobayashi M, Ikegami H, Fujisawa T, et al. Prevention and treatment of obesity, insulin resistance, and diabetes by bile acid-binding resin. Diabetes 2007;56:239–247
39. Prawitt J, Abdelkarim M, Stroeve JH, et al. Farnesoid X receptor deficiency improves glucose homeostasis in mouse models of obesity. Diabetes 2011;60:1861–1871
40. Watanabe M, Horai Y, Houten SM, et al. Lowering bile acid pool size with a synthetic farnesoid X receptor (FXR) agonist induces obesity and diabetes through reduced energy expenditure. J Biol Chem 2011;286:26913–26920
41. Li F, Jiang C, Krausz KW, et al. Microbiome remodelling leads to inhibition of intestinal farnesoid X receptor signalling and decreased obesity. Nat Commun 2013;4:2384
42. Jiang C, Xie C, Lv Y, et al. Intestine-selective farnesoid X receptor inhibition improves obesity-related metabolic dysfunction. Nat Commun 2015;6:10166
43. Kamegai J, Tamura H, Shimizu T, Ishii S, Sugihara H, Oikawa S. Effects of insulin, leptin, and glucagon on ghrelin secretion from isolated perfused rat stomach. Regul Pept 2004;119:77–81
44. Salem V, Izzi-Engbeaya C, Coello C, et al. Glucagon increases energy expenditure independently of brown adipose tissue activation in humans. Diabetes Obes Metab 2016;18:72–81
45. Tan TM, Field BC, McCullough KA, et al. Coadministration of glucagon-like peptide-1 during glucagon infusion in humans results in increased energy expenditure and amelioration of hyperglycemia. Diabetes 2013;62:1131–1138
46. Zhang Y, Ge X, Heemstra LA, et al. Loss of FXR protects against diet-induced obesity and accelerates liver carcinogenesis in ob/ob mice. Mol Endocrinol 2012;26:272–280
47. Lee CG, Kim YW, Kim EH, et al. Farnesoid X receptor protects hepatocytes from injury by repressing miR-199a-3p, which increases levels of LKB1. Gastroenterology 2012;142:1206–1217.e7
48. Joel CD. Stimulation of metabolism of rat brown adipose tissue by addition of lipolytic hormones in vitro. J Biol Chem 1966;241:814–821
49. Longuet C, Sinclair EM, Maida A, et al. The glucagon receptor is required for the adaptive metabolic response to fasting. Cell Metab 2008;8:359–371
50. Morris EM, Jackman MR, Meers GM, et al. Reduced hepatic mitochondrial respiration following acute high-fat diet is prevented by PGC-1α overexpression. Am J Physiol Gastrointest Liver Physiol 2013;305:G868–G880
51. Zhang Y, Castellani LW, Sinal CJ, Gonzalez FJ, Edwards PA. Peroxisome proliferator-activated receptor-gamma coactivator 1alpha (PGC-1alpha) regulates triglyceride metabolism by activation of the nuclear receptor FXR. Genes Dev 2004;18:157–169